Predicting Naphthenic Acid Migration Through the Foundation of Oil Sands Tailing Pond

Liang Ma · Cheng Huang ⬤ · Zhong-Sheng Liu

Abstract In this paper, a conceptual model was developed to predict the seepage of oil sands process-affected water with capabilities of evaluating the transport and attenuation of naphthenic acids through the dykes and the foundations of oil sands tailings pond. The model incorporates naphthenic acid diffusion, adsorption, dispersion, advection, and biodegradation, and was modeled through the commercial software tools to predict naphthenic acid fate in both spatial and time scales. The tailing pond of the Muskeg River Mine in the Athabasca oil sands deposit was investigated in the case study. The comparison between the onsite monitoring data and the simulation results was in good agreement. In addition, limiting factors for migration of naphthenic acid were also discussed based on a parametric sensitivity study.

1 Introduction

The extraction of crude oil from oil sands produces the oil sands process water (OSPW), which is eventually discharged into tailing ponds for storage. The OSPW contains traces of chemicals that are added in the production processes of oil sands and also chemicals that are extracted from oil sands, especially a complex mixture of organic acids—naphthenic acids (NAs) (Mackinnon and Boerger 1986; Clemente and Fedorak 2005; Grewer et al. 2010). The concentration of NAs in tailings ponds could be as high as 40 to 120 mg/L (Schramm et al. 2000). Predicting the migration of chemicals that exist in OSPW, particularly, NAs through the foundations of oil sands tailing ponds has become important to the design, the construction, and the use of oil sands tailing facilities. The prediction is also needed for designing mine site reclamation. The importance is partly due to the increasing volume of OSPW in tailing ponds. It is estimated that there will be over 1 billion m^3 of tailings that will require reclamation by 2025 (Quagraine et al. 2005).

As the migration and the fate of NAs in oil sand tailing facilities are of concern to oil sands producers, federal and provincial regulators, and also the public, many conceptual models have been developed to make evaluations and predictions. For example, predicting geochemical transport in field conditions by using conceptual models has been successfully validated in previous studies (Holden et al. 2013; Fala et al. 2013). Savard et al. (2012) simulated groundwater flow and used transport models to analyze the migration of chloride and metal ions under field conditions. In terms of NAs, onsite characterization work and field studies have been conducted on NA occurrence and fate in oil sand tailings (Headley and McMartin 2007). In addition, conceptual modeling started to make predictions on

L. Ma · C. Huang (✉) · Z.-S. Liu
Energy, Mining and Environment Research Center, National Research Council Canada, 4250 Wesbrook Mall, Vancouver, BC, Canada
e-mail: cheng.huang@nrc-cnrc.gc.ca

NA migration for oil sand tailing facilities. For example, Wang et al. (2013) did testing to extract NA transport properties and also used decoupled mass transport properties to simulate a simple 1D tailing pond, which shows the feasibility of using a prediction model. However, few full-scale modeling on NA migration has been done to interpret real field monitoring data at current stage.

In this paper, a modeling tool was developed to simulate the OSPW seepage flow in a 2D manner. In addition, all identified NA transport and attenuation mechanisms are fully coupled together, which enhanced the capabilities to precisely predict NA migration and fate in the foundation of oil sand tailing pond. In addition, a specific case study of the full-scale tailing pond at Muskeg River Mine site was performed to see if the proposed conceptual model can be validated. A multiparametric sweep was performed to calibrate key transport coefficients from the samples measured in lab conditions. Based on further sensitivity studies, the impact of limiting factors for NA migration was also discussed in the end.

2 Conceptual Model

The foundation of an oil sand tailing pond consists of several layers with different materials. To estimate OSPW seepage, the classic Darcy's law was applied to calculate the water flow velocity through each foundation layer:

$$\overline{\mathbf{u}} = -\frac{k_i}{\mu}\left(\nabla p - \rho \overline{\mathbf{g}}\right) = -K_i \nabla H \tag{1}$$

where $\overline{\mathbf{u}}$ is the OSPW seepage flow velocity, p is the water pressure in pore, $\overline{\mathbf{g}}$ is the gravity vector, H is the hydraulic head, μ is the dynamic viscosity of the water, and k_i and K_i denote permeability and hydraulic conductivity for the foundation layer constructed by material i, respectively.

Furthermore, Darcy's law was coupled with general mass transport equation (William 1998) in the regime of the porous foundation layers to investigate the migration and fate of NAs with the OSPW seepage flow. Here, the main identified transport and attenuation mechanisms for NAs in this study include adsorption, diffusion, dispersion, advection, and degradation.

As the seepage flow velocity is usually sufficiently low, the adsorption can be evaluated by the equilibrium

status when the species concentrations on the sorbent get balanced with the concentration in the solution phase. There are many equilibrium adsorption models that have been previously studied (Travis and Etnier 1981). In this study, a linear adsorption model was adopted as the NA concentration in OSPW is very low (Bayard et al. 1998)

$$k_{d,i} = \frac{c_{s,i}}{c} \tag{2}$$

where $k_{d, i}$ is the adsorption coefficient for NAs, $c_{s, i}$ is the NA mass that adsorbed on the surface of sorbent with unit mass, and c is the NA concentration in solution phase.

Diffusion is a kind of mass transport mechanism by spreading materials from high-concentration region to low-concentration region, which is the result of random molecular collision. Here, $D_{d, i}$ is the effective diffusion coefficient for NAs in the foundation layer built with material i, which is estimated as follows:

$$D_{d,i} = \frac{D\varepsilon_i}{\tau_i} \tag{3}$$

where D is the diffusion coefficient in solution phase, ε_i is the porosity, and τ_i is the tortuosity. For simplification, we used the widely accepted Millington and Quirk model to evaluate the tortuosity here.

$$\tau_i = \varepsilon_i^{1/3} \tag{4}$$

Dispersion is defined as the spreading material due to some irregular microscopic feature such as random distribution of pore size in porous medium. It is known that dispersion is often more significant than diffusion in advection-diffusion scenarios for porous medium. Here, $D_{e, i}$ is the dispersion coefficient for material i. Generally, the dispersion coefficient is proportional to the dispersity α_i and the magnitude of flow velocity U (Fel and Bear 2010).

$$D_{e,i} = \alpha_i U \tag{5}$$

Totally, the combination of diffusion flux and dispersion flux $J_{d, i}$ in porous material i can be deducted. Both of them are proportional to the negative of NA concentration gradient in solution phase.

$$J_{d,i} = -\left(D_{d,i} + D_{e,i}\right)\overline{\nabla}c \tag{6}$$

Another key transport mechanism is advection which means that species migrate with the fluid motion.

Specifically in this study, NA transports via OSPW seepage flow. So, the advection flux J_a can be specified as follows:

$$J_a = \overline{\mathbf{u}}c \tag{7}$$

Through literature review, we found that NAs are quite chemical stable and hard to interact with other processing chemicals added in oil sand extraction (Han et al. 2009). The NA degradation is mainly attributed to some kinds of microbial bacteria (Toor et al. 2013); thus, this mechanism is also called biodegradation. In addition, some NAs may undergo rapid photodegradation, but this kind of NA degradation is not considered here for the seepage flow, which is not under direct UV exposure. In real engineering practice, the biogeochemical reactions between NAs and bacteria are still too complicated to be fully determined. As a result, it is common to use the half-life of first-order reaction to simply evaluate the biodegradation rate of NAs (Headley et al. 2002).

$$R = c \times \frac{\ln(2)}{t_{1/2}} \tag{8}$$

where $t_{1/2}$ is the estimated half-life for NAs.

Based on mass conservation, we finally get the following mass transport equations for the migration of NAs with considering the OSPW seepage flow in the layer with material i.

$$\left(\varepsilon_i + \rho_{b,i}k_{d,i}\right)\frac{\partial c}{\partial t} + \overline{\nabla}\cdot\left(-\left(D_{d,i} + D_{e,i}\right)\overline{\nabla}c + \overline{\mathbf{u}}c\right)$$
$$= R \tag{9}$$

where $\rho_{b,i}$ is the bulk density for material i. On the interfaces between different foundation layers, the seepage flow velocity $\overline{\mathbf{u}}$ and the NA concentration in the solution phase c are considered to be consistent.

3 A Case Study for Muskeg River Mine

3.1 The Mine Site Description

The Muskeg River Mine is located between the Athabasca River and the Muskeg River in Alberta Canada. An open-pit mine is situated in the northern part of the mine site, and the tailing pond is located in the south of the mine site near the confluence of the two rivers. The tailing infrastructure of the Muskeg River Mine, which began operations in December 2002, was in this case study. All construction information about the tailing pond and monitoring data used for comparison and analysis come from open sources (Yasuda 2006; Yasuda et al. 2010).

The oil sands tailing pond at the Muskeg River Mine is enclosed by a ring tailings dyke. The foundation is an "overburden starter dyke" constructed with relatively impermeable materials called lean oil sands. As the water level in the tailing pond rose, the dyke was gradually raised and expanded over the starter dyke using the relatively coarse tailing sand from primary extraction. In the Muskeg River Mine, it is reported (Yasuda et al. 2010) that the Pleistocene sand (Pf-sand) and associated larger grain size granular are widely presented over the source of oil sands—McMurray Formation. In addition, many peat layers usually can be found over fluvial sand and gravel deposit in the Athabasca mine area. However, most of the peat layers in the Muskeg River Mine were removed before mining operation and only a small portion is left on site.

In this study, a cross section at the south of the tailing pond shown in Fig. 1 was selected for modeling. The first simulation is from December 2002 to October 2004 to calibrate the transport coefficients used in further simulation. The second simulation timeframe is set from October 2004 to May 2006 as onsite measurements are available to compare. There was no major dyke expansion construction during the second period. The configuration of the cross section for study is illustrated in Fig. 2. The tailing pond is located at the top right corner of the figure. The area in yellow denotes the body of the dyke which is constructed with coarse sand. The characterization from exploratory boreholes revealed that some of the boreholes struck thick (< 3 m) Pf-sand. For simplification, a Pf-sand layer with 3-m thickness (2 m in wet area) is assumed to be located on the top of the McMurray Formation foundation in the model. In addition, the structure of starter dyke built by lean oil sand and the several peat soil layers with approximately 3-m thickness has also been assumed.

In general, simulation of seepage of OSPW along with NA transport and attenuation was performed. Specifically, the NA diffusion, dispersion, advection, and biodegradation were integrated in the modeling. The commercial software COMSOL was used to build the fully coupled NA transport models.

Fig. 1 Satellite view of site in Dec 2004 (from Google Earth)
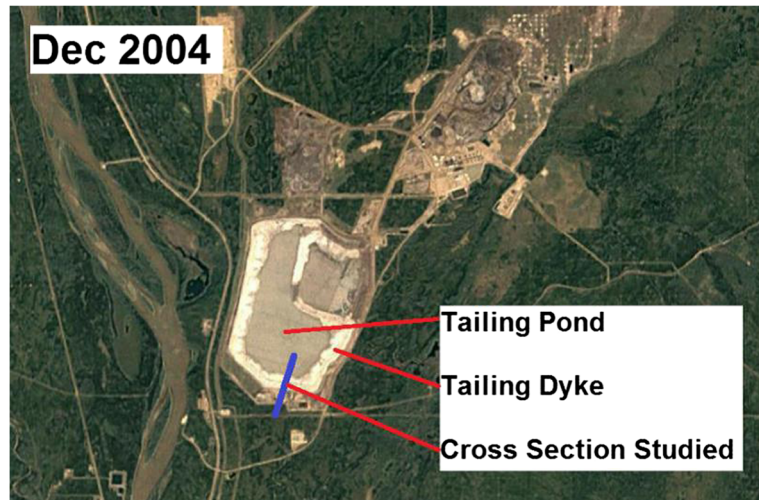
3.2 Hydrogeological Simulation

To simulate the OSPW seepage water, all physical properties of geologic materials and dyke materials were estimated by laboratory experiments and the typical value reported by Albian Sands Energy Inc. (ASE), the mining company. Monitoring data related to hydrogeology used in this study mainly come from the previous work by Yasuda (2006). In his primary modeling study, the studied section was divided into several domains by monitoring locations. The hydraulic modeling was simply estimated by separated 1D and 2D domains using the hydraulic heads from monitoring as boundary conditions. In our study, we integrated the studied section as a whole in 2D manner and apply the measured hydraulic heads only for the boundary conditions of two ending edges, which is able to make more reliable estimation of the seepage flow in the foundation layers. The calculated hydraulic head profile within the domain is used to compare with those monitoring data for model validation.

The hydraulic conductivity for the material in each foundation layer was estimated by characterization data given in Table 1. The anisotropy of hydraulic

conductivity was also considered in the modeling. Due to lack of water retention properties, nonlinearity of permeability was neglected and the Darcy's law was applied to calculate the seepage flow.

In terms of boundary conditions, the bottom surfaces of the McMurray Formation layer were defined as no flux for both of seepage and NA migration. Based on the hydraulic head profiles obtained from onsite monitoring, it was observed that precipitation seems to have very limited impact on the seepage for this site; thus, no recharge from precipitation was considered in the modeling. According to the measurement shown in Table 2, the hydraulic head boundary conditions on the bottom of tailing pond were set to 299.77 m which is measured onsite. However, there is a maximum 0.25-m hydraulic head difference at the outer ditch south during the monitoring period (2004–2006). As we focus on long-term (multiyears) rather than short-term (seasonal) hydraulic impact on NA migration, average groundwater velocity is sufficient to estimate the advection and dispersion of NAs through the foundation layers. Thus, the hydraulic head boundary conditions on the model left edge were set to 277.3 m. As a result,
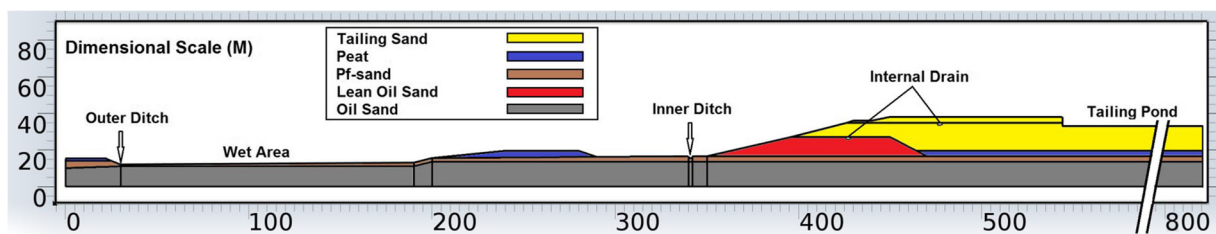

Fig. 2 Geometry configuration of the tailing pond of the Muskeg River Mine

Table 1 Hydraulic conductivity for each layer

No.	Domain	Materials	K_h (m/s)	Anisotropy (K_v/K_h)
1	Tailing dyke	Tailing sand	2e−5	0.1
2	Peat	Peat	9e−6	0.5
3	Pf-sand	Pf-sand	2e−4	1
4	Starter dyke	Lean oil sands	1e−8	0.5
5	McMurray Formation	Oil sands	2e−8	0.1

the discussion of the seepage flow in our model is simply assumed to be at steady state without considering any seasonal fluctuation.

In addition, the approximate average flow rate measured at the outtake drain pipes was estimated to be 0.6 L/s, which is mainly seepage water collected by internal drains. The drain pipe covers an approximately 150-m wide section of the dyke, so the discharge rate per meter length on the internal drains was estimated to be 4×10^{-3} L/s/m. The approximate average flow rate in the outer ditch was estimated to be 50 L/s. According to data reported by ASE, much of this outer ditch flow came from the dyke drain collected from inner ditch, and it was considered that only a small portion (< 5%) of the total flow rate in the outer ditch came from the discharge of the wet area. As an approximately 250-m wide section of the wet area is observed to contribute to the seepage into the outer ditch, the discharge rate per meter length on the surface of wet area was estimated to be < 0.01 L/s/m.

A parametric study on water discharge rates was performed to further calibrate the proposed OSPW seepage model. The model was calibrated by perturbing the water discharge rate on the bottom of inner ditch as currently no techniques are able to measure this rate. According to the onsite monitoring data, the discharge rate on the bottom of inner ditch is estimated to be 4×10^{-3} L/s/m. In our study, the perturbation of this discharge rate remains within a reasonable interval of a single order of magnitude from the initial values (from 0.1x to 10x). In addition, the water discharge rate into the wet area is also very difficult to measure or estimate onsite. As mentioned above, less than 5% of the total water flow rate in the outer ditch is estimated to be the discharge rate contributed by the wet area in previous study. Our preliminary calculation found that 5% of the total water flow rate is a little high, which is not able to generate a hydraulic head profile to match the onsite measured one. So, we also perturbed the water discharge rate ranging from 1 to 5% of total flow rate from the wet area into the outer ditch in our parametric study.

Based on the parametric study, the discharge rate on the bottom of the inner ditch was calibrated to 4×10^{-2} L/s/m, and the discharge rate into the wet area was calibrated to 4% of the total water flow rate measured from the outer ditch, as the scenario with these values shows the most similar pattern to what we found from the monitoring data. The contour of calculated hydraulic head and also the seepage flow direction are plotted in Fig. 3. The plotting shows that the main pathway for the seepage flow is from the bottom of tailing pond to the wet area. As shown in Table 2, the measured hydraulic head for the tailing pond and the outer ditch south were directly used as boundary conditions for the calculation; the hydraulic heads for the other 4 locations (inner ditch north, inner ditch south, wet area north, and outer ditch north) were used for

Table 2 Comparison of measured and calculated hydraulic head

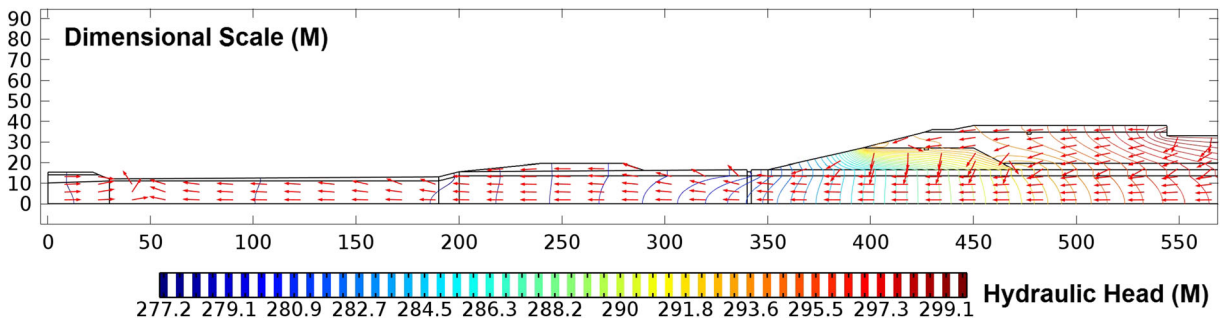| Locations	Measured head (m)	Calculated head (m)
Tailing pond (B.C.)	299.77	299.77
Inner ditch north (cross section)	High 280.23, low 279.98	280.63
Inner ditch south (cross section)	High 280.08, low 279.83	280.42
Wet area north (cross section)	High 277.61, low 277.58	277.50
Outer ditch north (cross section)	High 276.95, low 276.87	276.95
Outer ditch south (B.C)	High 277.44, low 277.19	277.3

Fig. 3 Calculated hydraulic head and seepage flow direction

comparison. The measured hydraulic heads show good agreement with the simulated results at these monitoring locations.

3.3 NA Transport and Attenuation

To fully investigate the NA transport and attenuation with OSPW seepage and their fate within the tailing pond infrastructure, the profile of seepage flow velocity calculated from hydrogeology modeling was imported to the advection term presented in Eq. (7).

Naphthenic acids are a diverse group of cyclopentyl and cyclohexyl carboxylic acids and are classified into several groups in terms of z value and n value. The former is related to the number of carbon rings in a molecule, and the latter is the carbon number of the molecule, thus proportional to the molecular mass (Rogers et al. 2002). At the Muskeg River Mine, the characterization and comparison of NAs based on z and n values showed that the group with $z = -4$ was the most common type (Yasuda 2006). In terms of molecular size, the n numbers 12 to 14 were most abundant species from tailings water. Further investigation indicates that all the samples from different locations have similar distribution of species. Yasuda provided measured NA concentrations in different monitoring locations from October 2004 to May 2006, as shown in Table 3. Some measurements in May 2006 are missing

Table 3 Measurement of NA concentration

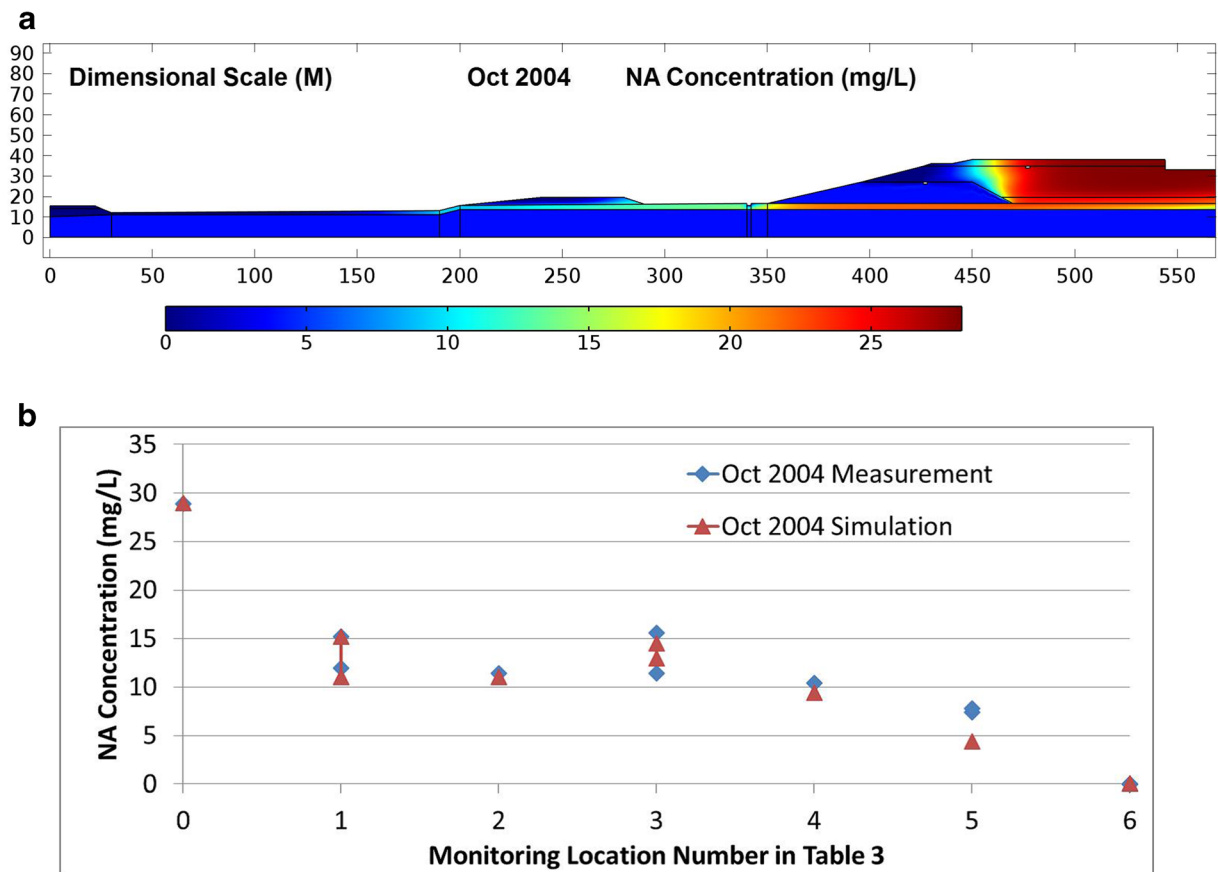| No.	Locations	Oct 2004 NAs (mg/L)	Jun 2005 NAs (mg/L)	May 2006 NAs (mg/L)
0	Tailing pond	28.9	29.3	–
1	Inner ditch north			
	Deep	15.2	14.7	–
	Mid	12.5	14.3	–
	Shallow	12.0	21.2	–
2	Inner ditch water	11.4	11.6	–
3	Inner ditch south			
	Deep	15.6	14.2	–
	Mid	15.5	13.8	–
	Shallow	11.4	13.4	–
4	Wet area north	10.4	11.3	–
5	Wet area			
	Measurement 1	7.4	8.1	9.7
	Measurement 2	7.8	–	10.3
6	Outer ditch south			
	Deep	< 1.0	< 1.0	–
	Mid	< 1.0	< 1.0	1.2
	Shallow	< 1.0	1.1	–

a

b

Fig. 4 NA concentration in Oct 2004. **a** Simulated NA concentration. **b** Comparison of measurement and simulation

as those of piezometer for collecting samples were demolished at that time. The boundary conditions for mass transport modeling in Eq. (9) include the inflow NA concentration at the bottom of the tailing pond was set to 29 mg/L based on the monitoring data from October 2004 and June 2005 shown in Table 3. The bottom of the inner ditch, the wet area, and also the model left edge were set to open boundary condition for NA transportation as follows:

$$
\begin{cases}
\mathbf{n} \cdot D_d \nabla c = 0 & \text{if } \mathbf{n} \cdot \overline{\mathbf{u}} \geq 0 \\
c = c_{\text{out}} & \text{if } \mathbf{n} \cdot \overline{\mathbf{u}} < 0
\end{cases}
\tag{10}
$$

where $\mathbf{n}$ denotes the normal vector of the boundary surface and c_{out} is the NA concentration for potential backflow, which is set to 0.1 mg/L (Savard et al. 2012). c_{out} for the bottom of the inner ditch was calculated instantly by combining NA concentration from two inner drains.

In terms of diffusion, it was assumed that the NAs have a uniform diffusivity 5×10^{-6} cm^2/s in the solution phase. The porosities for all material were approximately set to 0.3. In addition, the NAs were considered to be biodegraded in the foundation layers, and the half-life was set to be 3.9×10^4 days (Wang et al. 2013). The initial NA concentration in the McMurray Formation layer and starter dyke was defined as 4.4 mg/L, which was considered to represent the maximum contribution from the lean oil sands as background according to onsite observations. Regarding the adsorption term, it is found that the NA adsorption coefficient k_d may significantly correlated to the amount of bitumen doped on the sands. So k_d may range from 0 to 10 mL/g depending on the residual bitumen content. In this study, parametric studies were performed on the adsorption coefficients for the Pf-sand layer (low bitumen content) and also for the body of the dyke (high bitumen
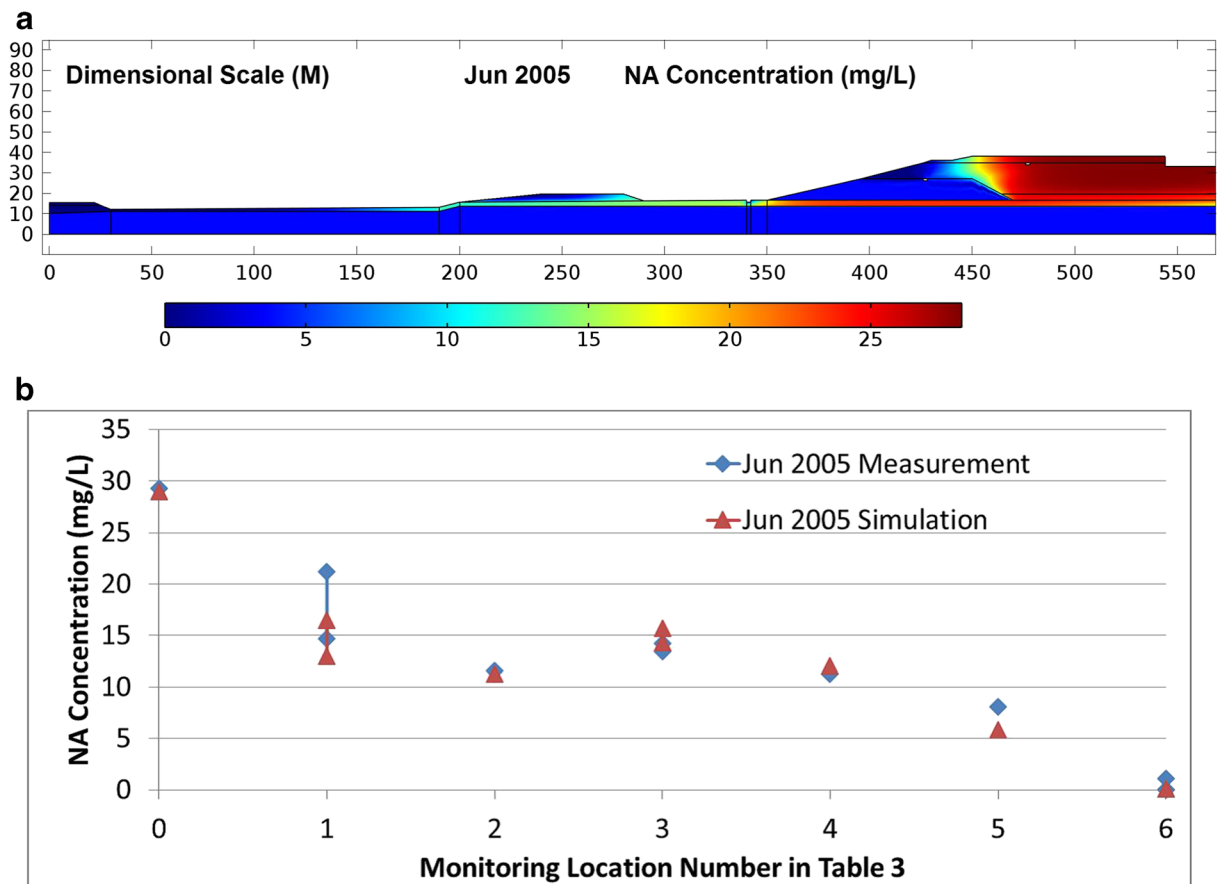
Fig. 5 NA concentration in Jun 2005. **a** Simulated NA concentration. **b** Comparison of measurement and simulation

content), where both of the adsorption coefficients were assumed to be in the range of 0.1 to 10 mL/g.

Due to the high heterogeneity of the dyke materials, the effect of dispersion was also considered in our models. The dispersion coefficient can usually be expressed as dispersity time flow rate according to Eq. (5). The previous characterization study from Wang (2013) shows that the NA dispersity for a similar sand material is 90 cm, which was based on a 10-cm lab column test. However, dispersity in the field is different from values measured in a laboratory, it is commonly observed that the dispersity is proportional to the scale of the geometry. As there is no characterization for the dispersity of the foundation layers in the Muskeg River Mine, another parametric study was performed on the NA dispersity based on the perturbation of Wang's measurement (from 0.1x to 10x). Consequently, two NA absorption coefficients for different layers as well as the NA dispersity, totally three parameters were swept simultaneously to calibrate NA transport and attenuation modeling in our study.

By comparing the simulation results from the parametric sweeping, it was determined that the absorption coefficient 0.1 mg/L for the Pf-sand layer, 0.2 mg/L for the body of the dyke, and also 0.1x for dispersity mean that dispersity 9 cm based on 10-cm column test makes the simulated NA concentration in October 2004 achieve a similar pattern measured from the field. All of above adjusted values were then used in the model as calibrated scenario for second calculation from October 2004 to May 2006.

The calculated contours of NA concentration from October 2004 to May 2006 for the calibrated scenario are plotted in Figs. 4,5,6. Moreover, comparisons between the simulation results and the
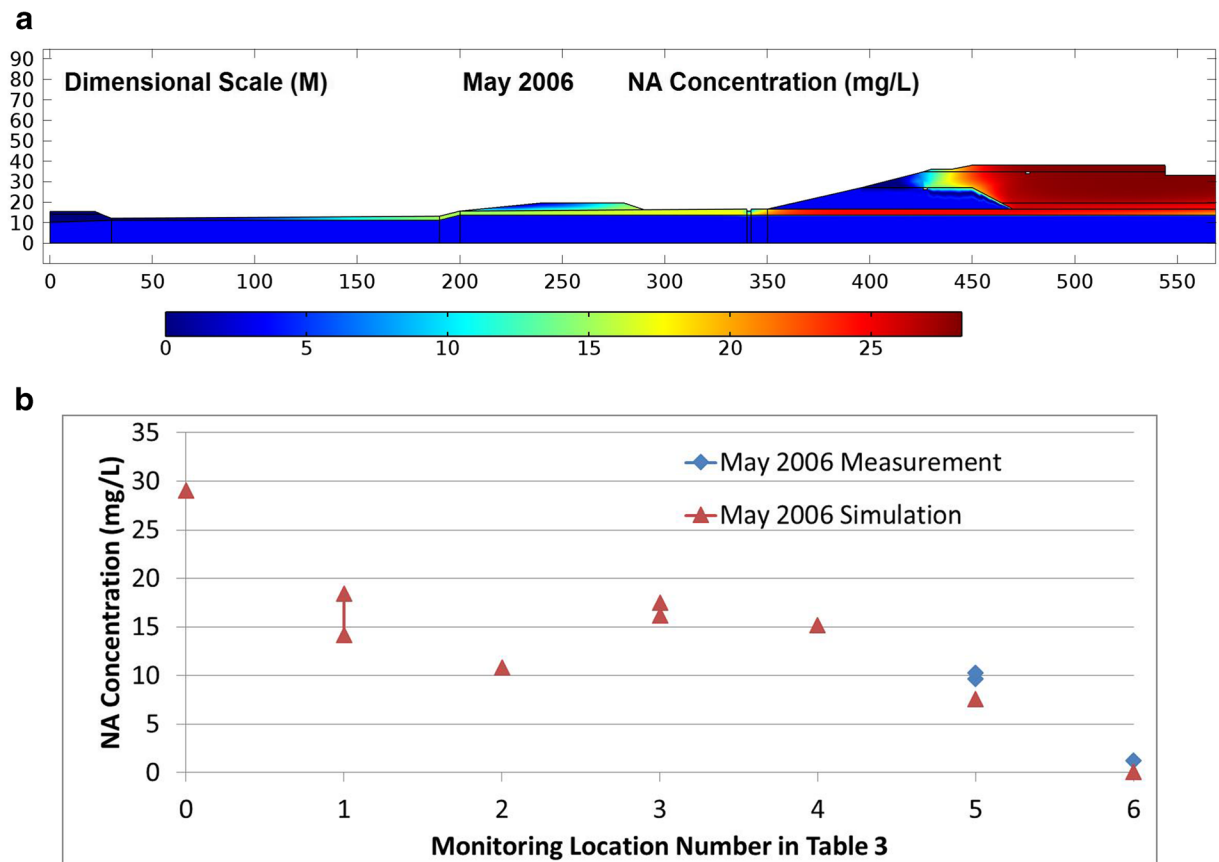
Fig. 6 NA concentration in May 2006. **a** Simulated NA concentration. **b** Comparison of measurement and simulation

measured ones are also given. In general, a good agreement is shown between the modeling and the measurement. Especially, the modeling results capture the gradient change of NA concentration

measured from the inner ditch area (no. 1 to no. 3). For the monitoring location far away from the dyke (no. 5 wet area and no. 6 outer ditch south), the simulated concentration seems a little below
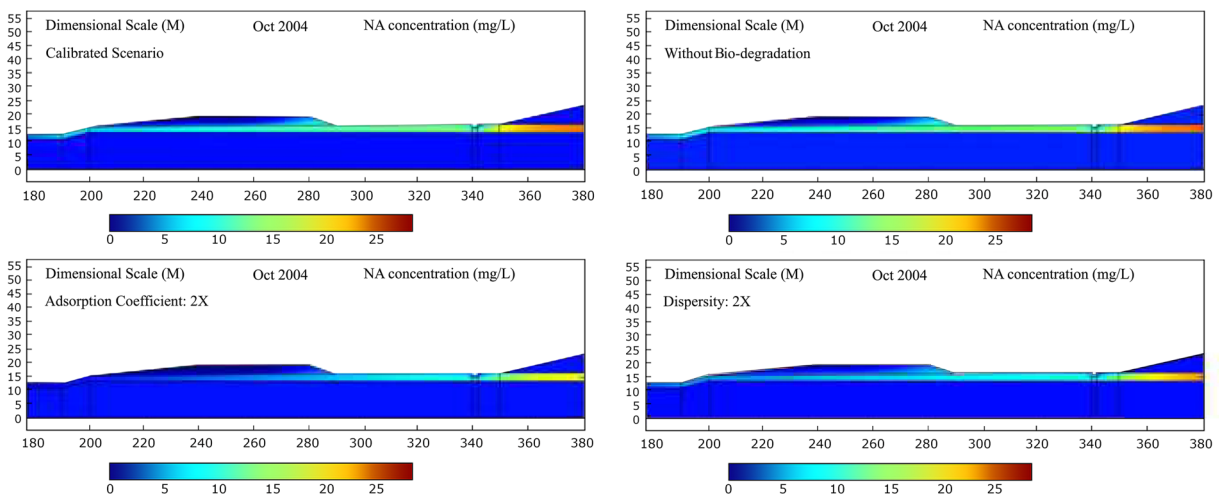

Fig. 7 Impact of biodegradation, adsorption coefficient, and dispersity

the measured value. A reasonable explanation is that the expansion of dyke was not considered and simulated in our study. This study assumed that the configuration had no change during the simulation period; however, the dyke body was gradually raised and expanded as the water level in the pond rose in operation practice, which made NAs may migrate further and faster during early operation period.

In conclusion, the observations on the simulation results from this case study show that the NA migration through the foundation of tailing pond in Muskeg River Mine is mainly via OSPW seepage in the Pf-sand layer. However, the simulations results from Fig. 3 predict that NAs should not be able to escape this tailing collection system due to the negative direction of seepage flow around the outer ditch region, which results from its hydraulic management design.

3.4 Sensitivity Study

In general, NAs are a complex mixture with a wide range of physical and chemical properties, and rates of biodegradation, adsorption, and dispersion depend in size and structure of NAs. For example, the rate of degradation is higher for lower molecular weight molecules having lower n values (Clemente et al. 2004). Through analyzing the simulation results of the parametric sweeping performed in the previous section, the sensitivities of three important transport and attenuation coefficients, biodegradation, adsorption rate, and dispersity, were also investigated to evaluate how the variation of these parameters impacts NA migration and fate. Figure 7 shows a comparison of NA concentration in the middle of our study area (from wet area to inner ditch) for four scenarios in October 2004. The top left contour is for the calibrated scenario obtained in Section 3.3; the top right is for the scenario without considering biodegradation; the bottom left is for the scenario with 2× adsorption coefficient, 0.2 mg/L adsorption rate for the Pf-sand layer, and 0.4 mg/L for the body of the dyke; the bottom right is for the scenario with 2x NA dispersity (18 cm based on 10-cm column testing).

From Fig. 7, it is found that there is no significant difference between the calibrated scenario and the scenario without biodegradation. The simulation results indicate that in this case study, natural NA biodegradation rate has limited impact in terms of

time scale on NA migration. This is consistent with the conclusions from a previous field study (Oiffer 2006). As a key attenuation mechanism, NA adsorption rate can significantly affect NA concentration and its migration in the field: a fairly higher adsorption capacity is able to bring aqueous concentrations lower. In addition, we also found that a higher dispersity also makes lower NA concentration status than the calibrated one. The reason we tend to attribute is that the higher dispersity makes more evenly distributed NA concentration in spatial scale, which may decrease the NA concentration gradient $\overline{\nabla} c$ in Eq. (6) and thus slows down the total diffusion and dispersion terms presented in Eq. (9).

4 Summary

In this paper, a new 2D conceptual model was developed to predict OSPW seepages and also evaluate the transport and the attenuation of NAs along the flow paths of OSPW. A full-scale case study of the tailing pond located at the Muskeg River Mine was conducted to test and refine the proposed model. The simulation results show good agreement with the onsite monitoring data in terms of hydraulic heads and NA concentration profiles. Moreover, the observation from our modeling results also reveals a potential pathway for NA migration and confirms the effectiveness of the tailing pond's hydraulic design to prevent NA migration into the environment. The sensitivities of transport coefficients were also studied, which provided us deeper understandings in the impact from variations of physical and chemical properties and the limiting factors for NA migrations. The limitation of this case study is that the calibration and refinement of the proposed model are based on limited available site data. Further calibration and refinement of the model with more monitoring data are desired. In the next step, we are improving the models' capabilities to simulate an expanding dyke body to better reflect the real operation practice in oil sand tailing ponds. The refined NA transport model coupled with hydraulic simulation can be applied to investigate the fates of other reactive contaminants, if the corresponding chemical interaction properties are available.

References

Bayard, R., Barna, L., Mahjoub, B., & Gourdon, R. (1998). Investigation of naphthalene sorption in soils and soil fractions using batch and column assays. *Environmental Toxicology and Chemistry, 17*, 2383–2390.

Clemente, et al. (2004). Aerobic biodegradation of two commercial naphthenic acids preparations. *Environmental Science and Technology, 38*, 1009–1016.

Clemente, J. S., & Fedorak, P. M. (2005). A review of the occurrence, analyses, toxicity, and biodegradation of naphthenic acids. *Chemosphere, 60*, 585–600.

Fala, O., Molson, J., Aubertin, M., Dawood, I., Bussière, B., & Chapuis, R. P. (2013). A numerical modelling approach to assess long-term unsaturated flow and geochemical transport in a waste rock pile. *International Journal of Mining Reclamation and Environment, 27*, 38–55.

Fel, L., & Bear, J. (2010). Dispersion and dispersivity tensors in saturated porous media with uniaxial symmetry. *Transport in Porous Media, 85*, 259–268.

Grewer, D. M., Young, R. F., Whittal, R. M., & Fedorak, P. M. (2010). Naphthenic acids and other acid-extractables in water samples from Alberta: what is being measured? *Science of the Total Environment, 408*, 5997–6010.

Han, X., MacKinnon, M. D., & Martin, J. W. (2009). Estimating the in situ biodegradation of naphthenic acids in oil sands process waters by HPLC/HRMS. *Chemosphere, 76*, 63–70.

Headley, J. V., & McMartin, D. W. (2007). A review of the occurrence and fate of naphthenic acids in aquatic environments. *Journal of Environmental Science and Health, Part A, 39*, 1989–2010.

Headley, J. V., Peru, K. M., Tanapat, S., & Putz, G. (2002). Biodegradation kinetics of geometric isomers of model naphthenic acids in Athabasca River water. *Canadian Water Resources Journal, 27*, 25–42.

Holden, A. A., Haque, S. E., Mayer, K. U., & Ulrich, A. C. (2013). Biogeochemical processes controlling the mobility of major ions and trace metals in aquitard sediments beneath an oil sand tailing pond: laboratory studies and reactive transport modeling. *Journal of Contaminant Hydrology, 151*, 55–67.

Mackinnon, M., & Boerger, H. (1986). Description of two treatment methods for detoxifying oil sands tailings pond water. *Water Quality Research Journal of Canada, 21*, 496–512.

Oiffer A (2006). Integrated solid phase, aqueous phase and numerical investigation of plume geochemistry at an oil sand mining facility. UWSpace. http://hdl.handle.net/10012/1210

Quagraine, E. K., Peterson, H. G., & Headley, J. V. (2005). In situ bioremediation of naphthenic acids contaminated tailing pond waters in the Athabasca oil sands region - demonstrated field studies and plausible options: a review. *Journal of Environmental Science and Health, Part A, 40*, 685–722.

Rogers, et al. (2002). Acute and subchronic mammalian toxicity of naphthenic acids from oil sand tailings. *Toxicological Sciences, 66*, 347–355.

Savard MM, Ahad JME, Gammon P, Calderhead AI, Rivera A, Martel R, Klebek M, Headley JV, Lefebvre R, Welsh B, Smirnoff A, Pakdel H, Benoit N, Liao S, Jautzy J, Gagnon C, Vaive J, Girard I, Peru K (2012). A local test study distinguishes natural from anthropogenic groundwater contaminants near an Athabasca oil sands mining operation. Public file Natural Resources Canada. https://doi.org/10.4095/292074

Schramm, L. L., Stasiuk, E. N., & MacKinnon, M. (2000). Surfactants in Athabasca oil sands slurry conditioning, flotation recovery and tailings processes. In L. L. Schramm (Ed.), *Surfactants, fundamentals and applications in the petroleum industry*. Cambridge: Cambridge University Press.

Toor, N. S., Han, X., Franz, E., MacKinnon, M. D., Martin, J. W., & Liber, K. (2013). Selective biodegradation of naphthenic acids and a probable link between mixture profiles and aquatic toxicity. *Environmental Toxicology and Chemistry, 32*, 2207–2216.

Travis, C. C., & Etnier, E. L. (1981). A survey of sorption relationships for reactive solutes in soils. *Journal of Environmental Quality, 10*, 8–17.

Wang, X., Robinson, L., Wen, Q., & Kasperski, K. L. (2013). Determination of thermodynamic and transport parameters of naphthenic acids and organic process chemicals in oil sand tailings pond water. *Environmental Science: Processes & Impacts, 15*, 1411–1423.

William DM (1998) Analysis of transport phenomena. New York: Oxford University Press.

Yasuda N (2006). Hydraulic performance of the seepage collection ditches at the Albian Sands Muskeg River Mine. UWSpace. http://hdl.handle.net/10012/2877. Accessed 31 Aug 2006.

Yasuda, N., Thomson, N. R., & Barker, J. F. (2010). Performance evaluation of a tailings pond seepage collection system. *Canadian Geotechnical Journal, 47*, 1305–1315.

Publisher's Note   Springer Nature remains neutral with regard to jurisdictional claims in published maps and institutional affiliations.